

Quantum compass interaction in post-perovskite iridate CaIrO_3

There is a new trend toward exploring Mott physics in 5d transition metal oxides with a strong spin-orbit interaction. Theoretical calculations using the Hubbard model revealed that the spin-orbit interaction drives a transition from a correlated metal to an insulator [1]. This novel Mott insulating state is actually realized in a layered perovskite, Sr_2IrO_4 , including Ir^{4+} ions with a $(t_{2g})^5$ electronic configuration [2]. In this compound, one hole among t_{2g} manifolds takes a complex wavefunction with the spin and orbital magnetic moments of $1/3$ and $2/3 \mu_B$, respectively, and this state is now called the $J_{\text{eff}} = 1/2$ state.

The superexchange interaction across two Ir^{4+} ions in the $J_{\text{eff}} = 1/2$ state is theoretically shown to be unique [3]. Although an antiferromagnetic Heisenberg interaction $J_1 \mathbf{S}_i \cdot \mathbf{S}_j$ is dominant in a corner-shared IrO_6 bond, the magnetic interaction of the edge-shared IrO_6 bond becomes highly anisotropic and ferromagnetic, i.e., $-J_2 \mathbf{S}_i^z \mathbf{S}_j^z$, where the z direction is perpendicular to the plane expanded by two Ir atoms and two O atoms responsible for the edge-shared bond. This interaction, which is called the quantum compass interaction owing to the analogy to the interaction between two compasses (Fig. 1), captures great interest since a quantum spin liquid is realized when this interaction occurs in the honeycomb lattice. To test the validity of this theory, it is necessary to elucidate the magnetic structure of an Ir oxide with both edge-shared and corner-shared IrO_6 bonds. We here focused on a post-perovskite-type compound, CaIrO_3 , which exhibits both edge-shared and corner-shared IrO_6 octahedral bonds [4]. The compound shows a Mott insulating behavior characterized by a charge gap of ~ 0.17 eV and undergoes a transition to a canted antiferromagnetic state at 115 K [5].

Resonant X-ray diffraction measurements were

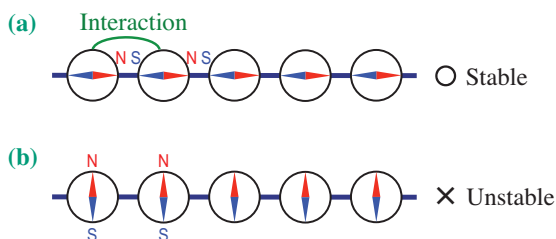


Fig. 1. Schematic of quantum compass model. When a number of compasses are placed in a line, they interact with each other, resulting in a stable state in which the N pole of a compass faces the S pole of the adjacent compass. The state in which the needles of the compasses point horizontally (Fig. 1(a)) is more stable in terms of energy than the state in which they point vertically (Fig. 1(b)). This anisotropic interaction is called the compass interaction. In the Heisenberg model, arrangement pattern (a) has the same energy as arrangement pattern (b).

performed at beamline **BL19LXU** (inset of Fig. 2(a)). An incident beam was monochromated by a pair of Si (111) crystals and irradiated on the (001) surface of the sample, which was placed in a ^4He closed-cycle refrigerator installed on a four-circle diffractometer with a vertical scattering plane geometry. The intensities of incident and scattered beams were detected by an ionization chamber and a Si PIN photodiode, respectively. The polarization of the incident beam was perpendicular to the scattering plane (σ) and that of the scattered beam was analyzed by using the (008) reflection of pyrolytic graphite.

Figure 2(a) displays the absorption spectra obtained by fluorescence measurements at room temperature as well as the energy dependence of the scattered intensity of the (005) reflection at 10 K. We can observe a strong resonance peak at the L_3 edge of ~ 11.21 keV. The space group of CaIrO_3 is $Cmcm$ with orthorhombic symmetry, where $(002n+1)$ reflections are forbidden according to the c -glide reflection. The polarization analysis indicates the π' character of the scattered beam (Fig. 2(b)). The temperature variation of the integrated intensity follows well that of the weak ferromagnetic moment (Fig. 2(c)). Considering also that the anisotropic tensor of susceptibility (ATS) scattering is prohibited in the measured geometry, we conclude that the observed reflection originates from a commensurate antiferromagnetic ordering. The observed magnetic reflections are well accounted for by considering an antiparallel arrangement of two Ir spins (labelled 1 and 2 in Fig. 3(a)) in a primitive unit cell. We can also determine the spin direction by representation analysis. The parasitic ferromagnetism along the b axis can be permitted only when the antiferromagnetic moments are along the c axis. The obtained magnetic structure is schematically drawn in Fig. 3. It has a stripe-type order with a parallel alignment along the a axis and an antiparallel alignment along the c axis.

Importantly, the magnetic reflection cannot be detected within the experimental accuracy at the L_2 -edge of ~ 12.82 keV, $I(L_2)/I(L_3) < 0.3\%$. This large edge dependence of the magnetic scattering intensity is interpreted on the basis of the ligand field theory. When the tetragonal crystal field Δ and spin-orbit coupling ζ are present, sixfold degenerated t_{2g} orbitals are split into three doubly degenerated bands. At the ground state, one hole occupies one of the highest energy orbitals

$$|\varphi_{\pm}\rangle = \frac{1}{\sqrt{A^2+2}} (A|x y \pm\rangle \pm |y z \mp\rangle + i|z x \mp\rangle).$$

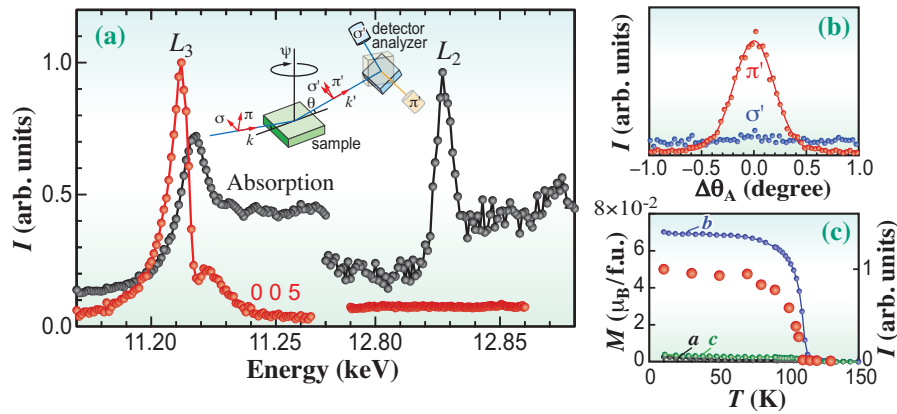


Fig. 2. (a) X-ray absorption spectra at room temperature and the magnetic scattering intensity (I) of the (0 0 5) reflection at 10 K near the Ir L -edge for CaIrO_3 . The inset shows a schematic view of the experimental configuration. (b) Polarization analysis of the scattered light at the L_3 edge, where θ_A is the analyzer angle. (c) Temperature (T) dependence of the magnetization (M) at 0.1 T and the intensity (I) of the (0 0 5) reflection. (f.u. = formula unit)

When one electron is virtually excited from the Ir $2p$ orbitals in a resonant process, the t_{2g} bands are fully occupied; this simplicity enables us to calculate the atomic scattering tensor straightforwardly. By combining contributions of two Ir sites in a striped-ordered state, we obtain the scattering intensity as a function of the A parameter. The scattering intensity ratio between the L_2 and L_3 edges can be written as

$$\frac{I(L_2)}{I(L_3)} = \frac{(A-1)^4}{(A^2-2A-2)^2}$$

By comparing with the experimental results, we can give a constraint $A > 0.61$ (a constraint $A > 0.87$ is deduced from the results of ATS scattering analysis). This result indicates that the orbital state of the $5d$ hole is close to the $J_{\text{eff}} = 1/2$ state.

The realization of the $J_{\text{eff}} = 1/2$ state in CaIrO_3 enables us to discuss the magnetic structure in a theoretical framework. The observed antiferromagnetic (ferromagnetic) interaction through the corner-shared (edge-shared) bonds is totally consistent with the theoretical predictions. Moreover, the weak ferromagnetism can be successfully explained theoretically. The anisotropic axis z in the quantum compass model is tilted from the crystallographic axis c by $\pm\alpha$ and distinguished between the Ir(1)-Ir(1) and Ir(2)-Ir(2) bonds (see Fig. 3); this distinct local anisotropic axis leads to spin canting toward the b axis. We therefore safely state that the quantum compass interaction occurs between the spins in CaIrO_3 . To the best of our knowledge, this is the world's first experimental demonstration of the quantum compass interaction for spins. Theoretically, arranging the spins that are subject to the quantum compass interaction in the honeycomb lattice is expected to enable the realization of Kitaev spin liquids, which can be used in quantum

computers. The achievement of our research is expected to markedly increase the likelihood of realizing spin liquids.

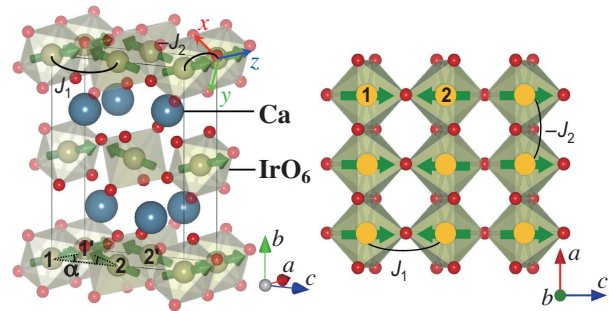


Fig. 3. Magnetic structure of post-perovskite-type compound CaIrO_3 . The magnetic moment is ordered in an antiparallel arrangement by the Heisenberg interaction denoted as J_1 and in a parallel arrangement by the quantum compass interaction denoted as J_2 . The magnetic moment is slightly tilted, which is caused by the anisotropy of the quantum compass interaction.

Kenya Ohgushi

Institute for Solid State Physics, The University of Tokyo

E-mail: ohgushi@issp.u-tokyo.ac.jp

References

- [1] D. Pesin and L. Balents: Nat. Phys. **6** (2010) 376.
- [2] B.J. Kim *et al.*: Science **323** (2009) 1329.
- [3] G. Jackeli and G. Khaliullin: Phys. Rev. Lett. **102** (2009) 017205.
- [4] K. Ohgushi, J. Yamaura, H. Ohsumi, K. Sugimoto, S. Takeshita, A. Tokuda, H. Takagi, M. Takata and T. Arima: Phys. Rev. Lett. **110** (2013) 217212.
- [5] K. Ohgushi *et al.*: Phys. Rev. B **74** (2006) 241104(R).